The Effect of Maleated Compatibilizers on the Structure and Properties of EVOH/Clay Nanocomposites

N. ARTZI, Y. NIR, *and* M. NARKIS*

Department of Chemical Engineering

and

A. SIEGMANN

Department of Materials Engineering
Technion-Israel Institute of Technology
Haifa 32000, Israel

The effect of compatibilizers on the blending torque, crystallization behavior, intercalation level, thermal stability and morphology of EVOH/treated clay systems was investigated. Maleic anhydride-grafted ethylene vinyl acetate (EVA-g-MA) or maleic anhydride-grafted linear low density polyethylene (LLDPE-g-MA) were used as compatibilizers of EVOH with clay, in various concentrations (1, 5 and 10 wt%). The blends were processed using Brabender Plastograph and characterized by XRD, SEM, DSC, DMTA and TGA. X-ray diffraction shows advanced intercalation within the galleries when the compatibilizers were added. Unique results were obtained for the EVOH/clay/compatibilizer systems, owing to a high level of interaction developed in these systems, which plays a major role. Thermal analysis showed that with increasing compatibilizer content, lower crystallinity levels result, until at a certain content no crystallization has taken place. Significantly higher viscosity levels were obtained for the EVOH/clay blends compared to the neat polymer, as seen by a dramatic torque increase when processed in the Brabender machine. The DMTA spectra showed lower T_g values for the compatibilized nanocomposites compared to the neat EVOH and the uncompatibilized composites. Storage modulus was higher compared to the uncompatibilized EVOH/clay blend when EVA-g-MA compatibilizer was added (at all concentrations), and only at low contents of LLDPE-g-MA. TGA results show significant improvement of the blends thermal stability compared to the neat EVOH, and to the uncompatibilized blend, indicating an advanced intercalation.

INTRODUCTION

The formation of polymer/organoclay nanocomposite was reviewed by Lagaly (1), Akelah (2), Giannelis (3), Pinnavaia (4) and Mülhaupt (5). Such nanocomposites may exhibit unique property combinations, e.g., higher heat distortion temperature combined with higher stiffness, strength, and improved barrier properties. Recently, improved flame retardency was also attributed to nanocomposite formation. A number of parameters play a role in the process of nanocomposites formation in the melt, i.e., ammonium cation used in cation exchange, processing temperature, level of shear rate, compatibilizer type and content, and polymer viscosity (6). A layered silicates uniformly dispersed in a polymer matrix are desired to improve performance. However, despite the high aspect ratio of the silicate individual layers, they are not easily dispersed in most polymers, owing to the preferred state of face-to-face stacking in the agglomerated tactoids. Disintegration of the tactoids into discrete monolayers may be further hindered by the intrinsic incompatibility of hydrophilic-layered silicates and hydrophobic engineering plastics. The replacement of the inorganic exchanged cations in the galleries of the native clay by

*Corresponding author. Email: narkis@tx.technion.ac.il

alkylammonium surfactants can compatibilize the surface of the clay with an hydrophobic polymer matrix (7).

Compatibilization is a common method to mediate an attractive interaction between phases, enhancing formation of the desired morphology and the associated mechanical properties. In general, compatibilizers reduce interfacial tension; hence increase interphase adhesion, leading to a finely dispersed morphology, and stability against gross segregation. Compatibilizers are often based on functionalized polyolefins with acrylic acid (8, 9), maleic anhydride (10, 11), or other modified thermoplastics with polar groups such as ionomers (12, 13). Maleic anhydride-grafted polyethylene, MA-g-PE, has been used as a compatibilizer in immiscible polymer blends such as EVOH/PE (14). Development of covalent bonds through the reaction of anhydride groups with the EVOH hydroxyl groups forms an *in-situ* EVOH-g-PE. The EVOH/PE blends exhibited increased melt viscosity and storage modulus and also enhanced tensile properties with the addition of MA-g-PE, which helps generate particle size reduction and improved interfacial adhesion.

Polymer intercalation is known to depend on the presence of polar interactions between the polymer chains and the clay. The silicate layers of the clay have polar hydroxy groups and are incompatible with polyolefin. Hence, PP/clay nanocomposites are prepared by using a functional oligomer as compatibilizer, such as maleic anhydride-modified PP oligomer (15). Even when polar polymers such as epoxy are used, nanocomposites may exhibit shortcomings in some properties such as tensile strength, which decreases with increasing silicate content. This behavior could result from inadequate interfacial adhesion. In order to improve interfacial adhesion compatibilizers were added (16).

A recent study regarding melt mixing of EVOH with clay under dynamic conditions (17) revealed that in spite of the high interaction level between the polar EVOH and the treated clay, which has led to a mixed intercalation and delamination morphology, some mechanical properties were deteriorated. The main reason suggested was a dramatic decline of EVOH crystallinity level, owing to interruption of crystallization caused by the high EVOH/clay interaction level. In addition, the low molecular weight onium ions treating the clay, may locally plasticize the EVOH matrix when delamination occurs.

In an attempt to improve the interaction level between the EVOH matrix and the clay tactoids, and simultaneously increase the level of intercalation and exfoliation, different compatibilizers were used. This study focuses on the influence of compatibilizers, i.e. maleic anhydride-grafted EVA, EVA-g-MA, or maleic anhydride-grafted LLDPE, LLDPE-g-MA, and processing conditions on the resulting EVOH/clay nanocomposite morphology, intercalation/exfoliation levels, and the thermal and dynamic mechanical behavior. The EVOH/clay proportion 85/15 was selected, as in previous works (17, 18), in order to magnify the phenomena observed. Much lower clay concentrations are currently studied aiming at the development of useful physical properties of EVOH/clay nanocomposites.

EXPERIMENTAL

Materials

The EVOH used in this study is a commercial product of Kuraray, Japan, containing 32 mole% ethylene. The treated clay used is Nanomer-1.30E clay, an onium ion modified montmorillonite mineral, obtained from Nanocor, Illinois. This organo-clay contains 70–75 wt% montmorillonite and 25–30 wt% octadecylamine. It is said to be designed for ease of dispersion in amine-cured epoxy resins to form nanocomposites. Two types of compatibilizers were studied: EVA-g-MA (maleic anhydride-grafted ethylene vinyl acetate), Orevac as a trade name, from Atofina, France, and LLDPE-g-MA (maleic anhydride-grafted linear low density polyethylene) from Mitsui, Japan. Both contain less than 2 wt% MA.

Preparation Methods

Prior to melt blending, the EVOH was ground into a powder. The polymer and clay powders were dried in vacuum at 80°C and 60°C, respectively, for 15 h. The components were dry-blended at selected ratios, and subsequently melt-mixed, in a Brabender plastograph machine, equipped with a 50 cm^3 cell, at 230°C and 60 rpm. The blends contained 15 wt% clay and different amounts (1, 5, 10 wt%) of EVA-g-MA or LLDPE-g-MA. An uncompatibilized 85/15 EVOH/clay sample was also prepared for comparison. All the resulting blends were compression molded at 230°C and 1000 MPa into 3-mm-thick plaques and subsequently characterized.

Characterization

Differential scanning calorimetry (DSC) was employed to characterize the thermal behavior of the composites. A Mettler DSC 30 system, under nitrogen atmosphere, at a heating rate of 10°C/min was used. Samples were heated to a temperature above their melting, cooled at the same rate, and subsequently reheated. The melting behavior was determined from the second heating run. Dynamic mechanical properties of the compression-molded samples were measured using a dynamic mechanical thermal analysis system (DMTA, Perkin Elmer Series 7), in the three point bending mode. The system was operated at 1 Hz, under nitrogen atmosphere, at a heating rate of 3°C/min. The structure of the composites was examined by a Philips X'PERT system X-ray diffraction (XRD), with a CuKα radiation source operated at 40 kV, 40 mA at a scanning rate of 0.5°/min. The blends' phase morphology was studied by electron microscopy. A Jeol JSM 5400 scanning electron microscope (SEM) was employed for observation of freeze-fractured and

microtomed surfaces. All samples were gold sputtered prior to observation. The samples were further characterized using a TA Thermogravimetric Analyzer (TGA) 2050. Samples were heated under an air atmosphere, at a heating rate of 20°C/min, and their weight loss was monitored.

RESULTS

Brabender Compounding

EVOH/clay mixtures were melt blended in a Brabender Plastograph cell. *Figure 1a* shows the mixing torque as a function of mixing time for the systems containing the EVA-g-MA as a compatibilizer. The plastograms are affected by the EVA-g-MA content and show an abrupt torque upturn. The viscosity of EVA-g-MA containing 15 wt% clay is low and slightly decreases with time. When 1 wt% EVA-g-MA is added to EVOH containing 15 wt% clay, the torque rise is delayed compared to the reference 85/15 EVOH/clay system. However, using 5 and 10 wt% EVA-g-MA shortens the time for the torque to rise by 15 and 18 min, respectively. The neat EVOH, neat EVA-g-MA and blends containing the same amounts of EVA-g-MA (without clay, not shown here) show a stable constant torque as a function of mixing time. Although the EVA-g-MA viscosity is much lower than that of neat EVOH, EVOH containing 1 wt% EVA-g-MA has higher viscosity than the neat EVOH. For higher EVA-g-MA contents, the torque level decreases. The sharp torque decrease seen after 40 min of mixing when 10 wt% compatibilizer was incorporated, in the presence of 15 wt% clay, is a result of mechanical grinding into powder of the hot mass under the dynamic mixing conditions.

Figure 1b shows mixing torque as a function of mixing time for the corresponding systems containing LLDPE-g-MA as a compatibilizer. The viscosity of LLDPE-g-MA containing 15 wt% clay is also low and decreases with time, as for EVA-g-MA. The same trend of torque upturn is noticed after shorter times by comparison to the reference 85/15 EVOH/clay blend. However, the torque decrease is seen already for the 5 wt% compatibilizer (compared to 10 wt% in the former case). The blends containing different amounts of compatibilizer based on LLDPE in the absence of clay (not shown here), showed constant torque values with time, similar to the EVA-g-MA compatibilizer systems. Although LLDPE-g-MA viscosity is similar to that of neat EVOH and therefore, higher than that of EVA-g-MA, the blends containing the same amounts of compatibilizers exhibited lower torque values when LLDPE-g-MA was used.

XRD

X-ray diffraction is a conventional method to characterize the gallery height in clay particles, which is indicative of their extent of intercalation. *Figure 2* shows the X-ray diffraction pattern of neat clay, [85/15 EVOH/clay], and blends containing EVA-g-MA as compatibilizers. The increase in the clay basal spacing in the presence of EVOH is higher for the compatibilized systems, and is more significant for larger compatibilizer amounts. The neat clay shows a characteristic peak at $2\theta = 3.58°$ ($d_{001} = 25Å$). The incorporation of 15 wt% clay into EVOH has resulted in an intercalated structure with a gallery spacing of 32Å ($2\theta = 2.72°$). Reference samples of 85/15 EVA-g-MA/clay and 85/15 LLDPE-g-MA/clay were examined in order to characterize the tendency of each compatibilizer by itself to intercalate, showing significantly different gallery heights of 42 and 29Å, respectively. The EVOH/clay systems containing 1, 5 and 10 wt% EVA-g-MA exhibit characteristic peaks at 2.6, 2.5 and 2.3° (d_{001} = 33, 35 and 38Å), respectively. The gallery heights of the corresponding blends containing LLDPE-g-MA are 34, 35 and 38Å, respectively, same as obtained for the EVA-g-MA. Although EVA-g-MA itself tends to intercalate more than LLDPE-g-MA and more than EVOH, the final gallery heights were similar for the two compatibilizers.

SEM

Observation of cryogenically fractured surfaces was performed by SEM. The morphology of the immiscible reference blends without clay, i.e. [95/5 EVOH/EVA-g-MA] and [95/5 EVOH/LLDPE-g-MA] are presented in *Fig. 3*. The compatibilizer's particles are smaller for the grafted EVA (*Fig. 3a*) than for the grafted LLDPE (*Fig. 3b*). In both cases, the compatibilizer particle size increases (not shown here) with compatibilizer concentration.

Figure 4 depicts the morphology of EVOH/clay/compatibilizer systems. *Figure 4a* shows the (85/15 EVOH/clay) system where the clay particles are difficult to distinguish. However, the brighter areas seem to present clay particles, composed of bimodal, large aggregates of size greater than 10μ and small particles of less than 1μ. The [80/15/5 EVOH/clay/EVA-g-MA] system (*Fig. 4b*) has a developed structure compared with that of the uncompatibilized system (*Fig. 4a*) and the clay particles are hardly observable.

Figure 4c depicts the [75/15/10 EVOH/clay/EVA-g-MA] system, where clay particles cannot be observed. The same general trends are observed for the LLDPE-g-MA systems (not shown here). However, the clay particles are more clearly observed in the presence of this compatibilizer compared to the EVA-g-MA compatibilizer. The clay particles seen are larger and less adhered to the matrix.

Figure 5 depicts room temperature microtomed surfaces of the [75/15/10 EVOH/clay/EVA-g-MA] and [75/15/10 EVOH/clay/LLDPE-g-MA] systems. Highly stretched fibrils crossing the cracks formed are seen in both systems. The observed voids may represent clay particles that have been pulled out by microtoming. One can see by the size of the voids that the clay particles are larger in the case of LLDPE-g-MA (*Fig. 5b*)

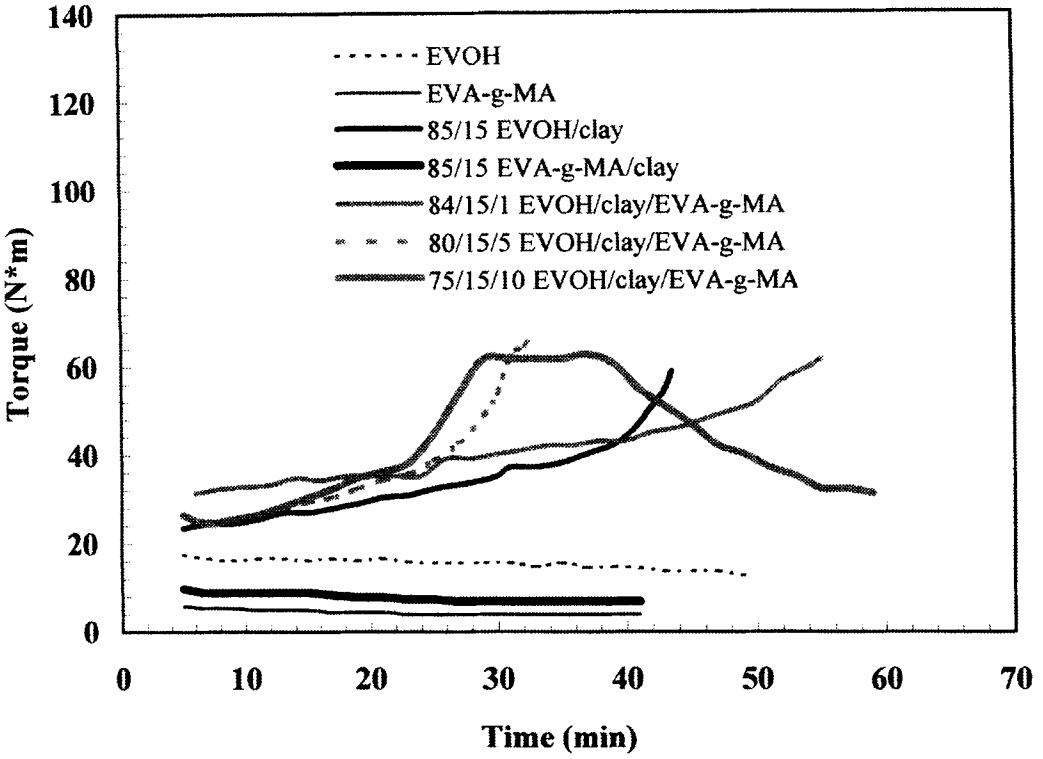

Fig. 1a. Brabender plastograms of EVOH/clay systems containing EVA-g-MA, at 230°C and 60 rpm.

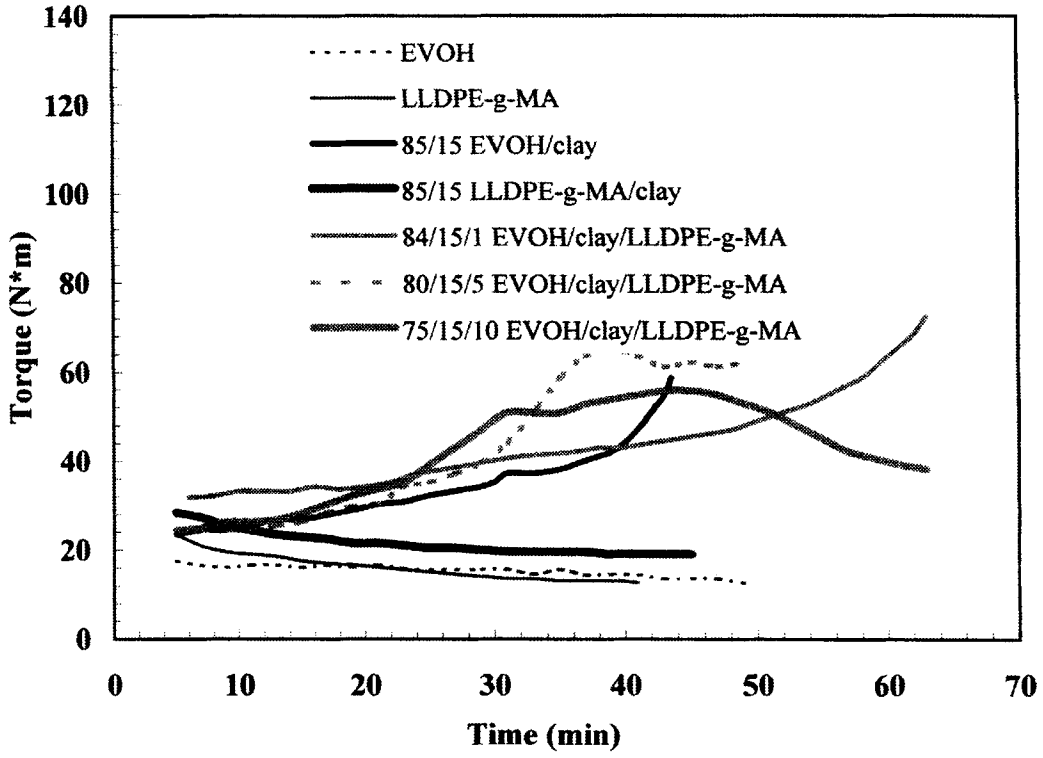

Fig. 1b. Brabender plastograms of EVOH/clay systems containing LLDPE-g-MA, at 230°C and 60 rpm.

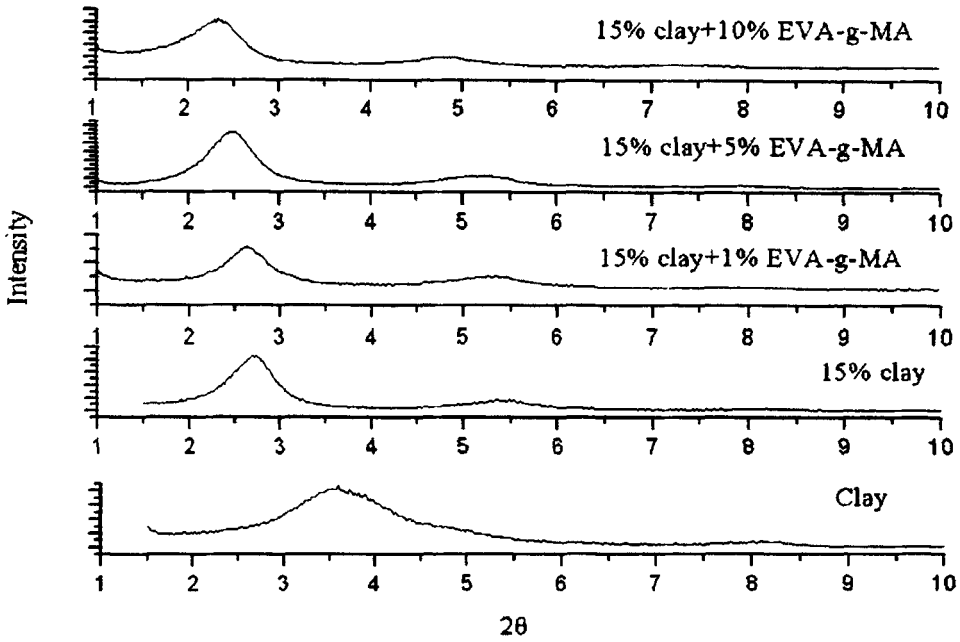

Fig. 2. X-ray diffraction patterns of EVOH/clay systems containing EVA-g-MA.

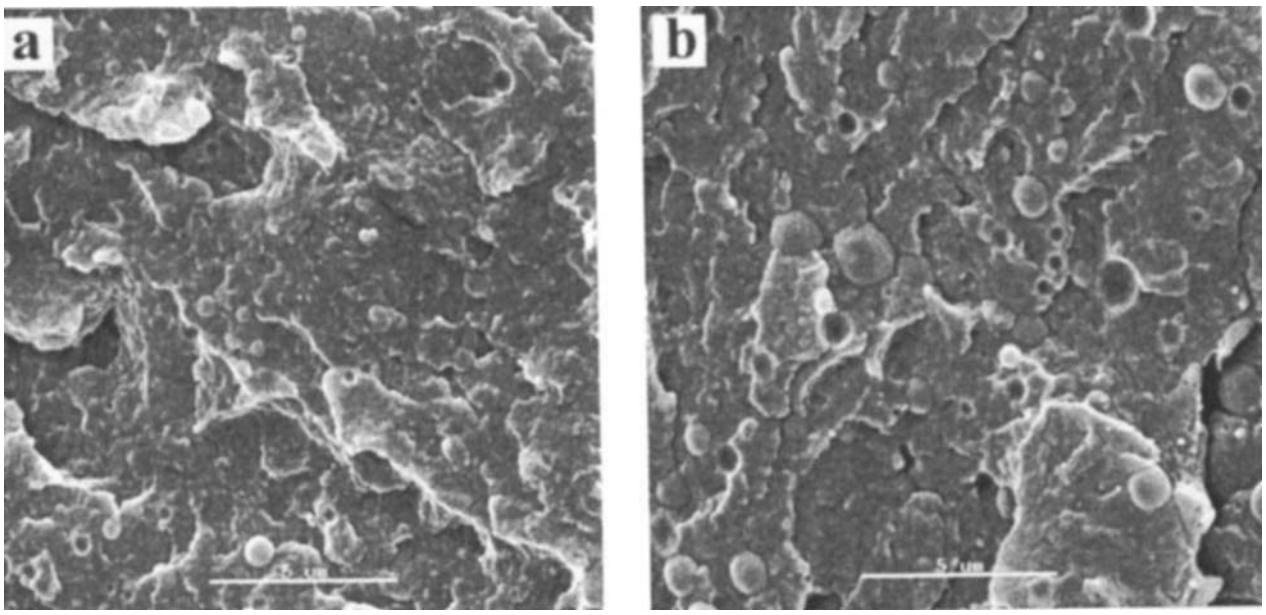

Fig. 3. SEM micrographs of freeze-fractured surfaces of EVOH/compatibilizer blends: (a) [95/5 EVOH/EVA-g-MA], (b) [95/5 EVOH/LLDPE-g-MA].

compared with EVA-g-MA (*Fig. 5a*), in agreement with micrographs of freeze-fractured surfaces.

DSC

DSC results of neat EVOH, [85/15 EVOH/clay] and blends containing EVA-g-MA are presented in *Table 1*. Significant changes in the EVOH melting behavior are observed, which are more significant for higher amounts of the EVA-g-MA compatibilizer. The thermal characteristics of the EVOH containing different amounts of EVA-g-MA, without clay, are similar to those of the neat EVOH (not shown here). When clay is incorporated, the melting temperatures (T_m) of 84/15/1 and 80/15/5 EVOH/clay/EVA-g-MA (166 and 160°C, respectively) are higher compared to that of the uncompatibilized 85/15 EVOH/clay blend (156°C). However, the reduction of the melting temperature compared to the neat EVOH (180°C) is significant.

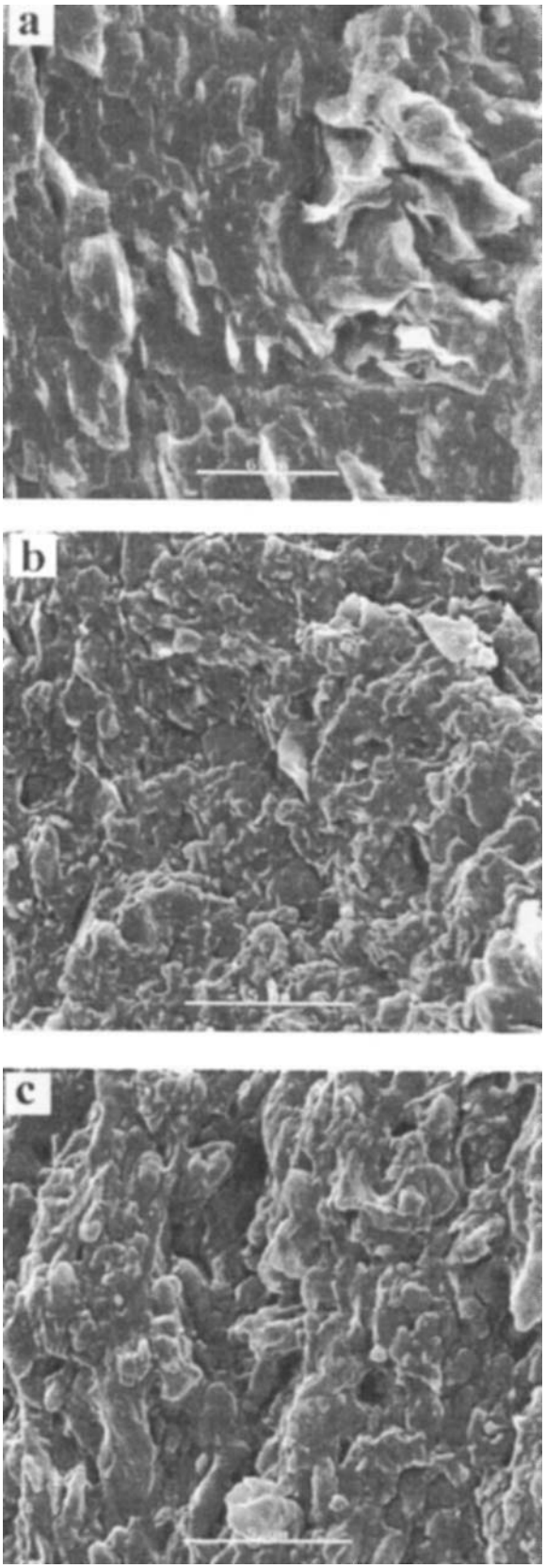

Fig. 4. SEM micrographs of freeze-fractured surfaces of (a) [85/15 EVOH/clay]. (b) [80/15/5 EVOH/clay/EVA-g-MA], (c) [75/15/10 EVOH/clay/EVA-g-MA].

Interestingly, at 10 wt% EVA-g-MA, no melting peak is observed, indicating the absence of crystalline phase in this case. The reduced crystallinity, as presented by the heat of fusion, is also higher for the blends containing 1 and 5 wt% compatibilizer compared to the uncompatibilized blend (41, 34 and 32 mW/g, respectively). Similar trends were observed for the crystallization process (*Table 1*).

The [84/15/1 EVOH/clay/LLDPE-g-MA] blend shows less interruption to the EVOH crystallization process (*Table 1*). However, when 5 wt% LLDPE-g-MA was used, the interruption was significant and for 10 wt% LLDPE-g-MA no crystallization has occurred.

DMTA

The effect of the compatibilizers on the dynamic mechanical properties of neat EVOH, in the absence of clay, was first studied. *Figures 6a* and *6b* depict the storage modulus curves of EVOH containing 1, 5 and 10 wt% EVA-g-MA and LLDPE-g-MA, respectively. It can be seen that the compatibilizer type plays an important role in determining the dynamic moduli. When EVA-g-MA was added, the glassy state modulus increased compared to the neat EVOH at all studied compatibilizer concentrations (*Fig. 6a*). The increase was less significant for the higher compatibilizer loadings. However, for LLDPE-g-MA, *Fig. 6b*, reduction in the modulus compared to the neat EVOH has occurred for the same loadings. Moreover, as the compatibilizer content increases there is a decrease in the moduli in both cases, i.e. for EVA-g-MA and LLDPE-g-MA.

The storage moduli of the EVOH/clay/compatibilizer systems, at different contents of EVA-g-MA and LLDPE-g-MA, are depicted in *Fig. 7*. The glassy storage modulus of EVOH containing 15 wt% clay is lower than that of the neat EVOH (*Fig. 7a*). Upon compatibilizer addition at 1 and 5 wt%, the modulus increases. At 10 wt% EVA-g-MA, however, the modulus decreases and is lower than the neat polymer's modulus. For LLDPE-g-MA (*Fig. 7b*), incorporation of 1 wt% compatibilizer resulted in a slight modulus increase compared to the uncompatibilized blend containing 15 wt% clay, but the modulus was lower than that of the neat polymer.

T_g values were obtained from the loss modulus curves of the blends. Incorporation of EVA-g-MA without clay resulted in T_g values higher than that of neat EVOH by 3.5°C for 1 wt%, and similar T_g values for 5 and 10 wt%. Adding 1 wt% LLDPE-g-MA, without clay, yielded lower T_g by 4°C, and for 5 and 10 wt% T_g was similar to the neat EVOH (not shown here). The glass transition temperatures of the 85/15 EVOH/clay and the neat polymer are similar. Incorporation of compatibilizer in addition to clay, resulted in reduction of 9°C for 10 wt% EVA-g-MA and reduction of 3°C and 11°C for 5 and 10 wt% LLDPE-g-MA, respectively (*Table 2*).

TGA

Table 3 summarizes TGA under air experiments for neat EVOH, neat compatibilizers, [85/15 EVOH/clay]

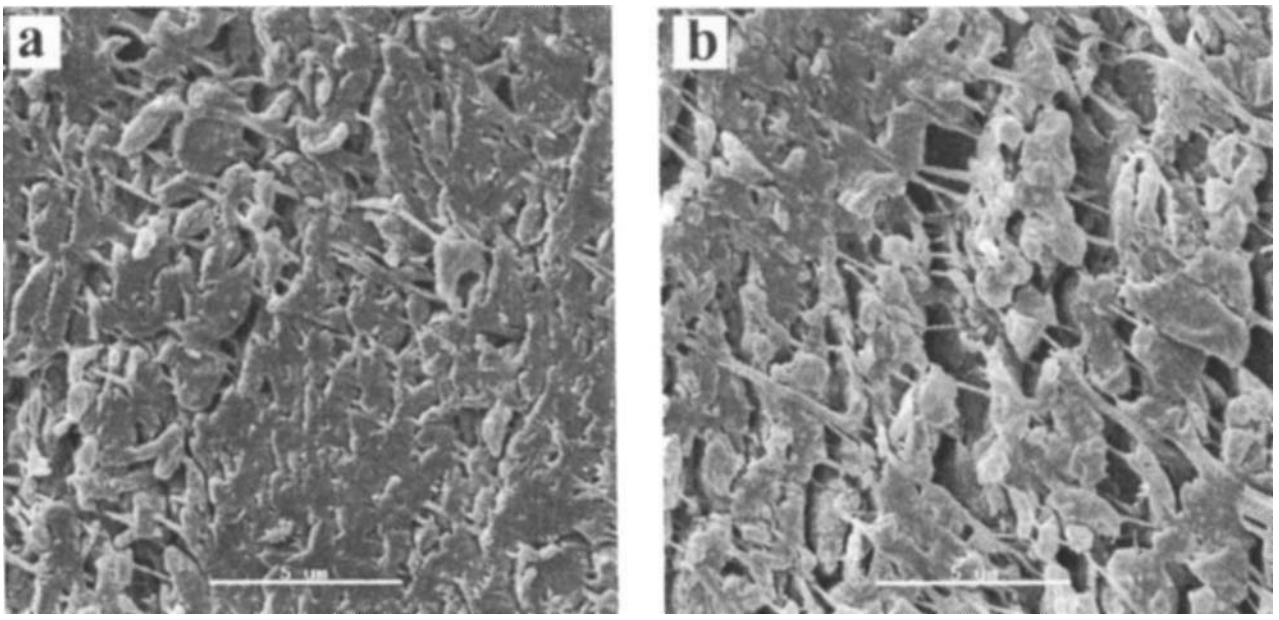

Fig. 5. SEM micrographs of microtomed surfaces of EVOH/clay/compatibilizer: (a) [75/15/10 EVOH/clay/EVA-g-MA], (b) [75/15/10 EVOH/clay/LLDPE-g-MA].

Table 1. Thermal Characteristics of EVOH/Clay/Compatibilizer Nanocomposite Systems Containing EVOH and 15 wt% Clay.

	Tc (°C)	ΔHc (mW/g)	Tm (°C)	ΔHm (mW/g)
EVOH	160	60	180	82
EVOH + 15% clay	143	29	156	32
1% EVA-g-MA	158	35	166	41
5% EVA-g-MA	132	30	159	34
10% EVA-g-MA	—	0	—	0
1% LLDPE-g-MA	157	30	162	35
5% LLDPE-g-MA	98	15	135	20
10% LLDPE-g-MA	—	0	—	0

and the compatibilized blends containing 1, 5 and 10 wt% of both types. The compatibilizers play an important role in determining the thermal stability of the blends. The decomposition temperature of neat EVOH is 404°C (determined at 50% mass loss). The decomposition temperature increases when the compatibilizer is added to the neat polymer at all contents for both types. The decomposition temperature increases to 424°C when 15 wt% clay is added to the neat polymer. When different amounts of compatibilizer are added in addition to the 15 wt% clay, the decomposition temperatures significantly increase, for both compatibilizers. The maximum increase of decomposition temperature, compared to the neat polymer, i.e. 50°C, has occurred for the [75/15/10 EVOH/clay/EVA-g-MA] system.

DISCUSSION

The compatibilizers affect both the neat polymer in the absence of the clay and the structuring process of the nanocomposites because of their high interaction level with the EVOH and the clay. To help analyze the foregoing results, the main trends are summarized in *Table 4*.

The effect of the compatibilizers on the neat EVOH (no clay) was observed by the torque level in the Brabender plastograph (not shown here). Apparently, the formation of intermolecular hydrogen bonds between the hydroxyl (strong proton donating group) and maleic anhydride groups of both compatibilizers (proton accepting) (19) during the melt mixing process is sufficiently high to increase the EVOH viscosity. The viscosity of the blends increased compared to the neat EVOH when 1 wt% compatibilizers of both types were used. In the case of EVA-g-MA, intermolecular hydrogen bonds may be formed also with the vinyl acetate group. Therefore, although the viscosity of EVA-g-MA is lower than that of both EVOH and LLDPE-g-MA, the blends containing EVA-g-MA exhibited higher torque than that containing LLDPE-g-MA

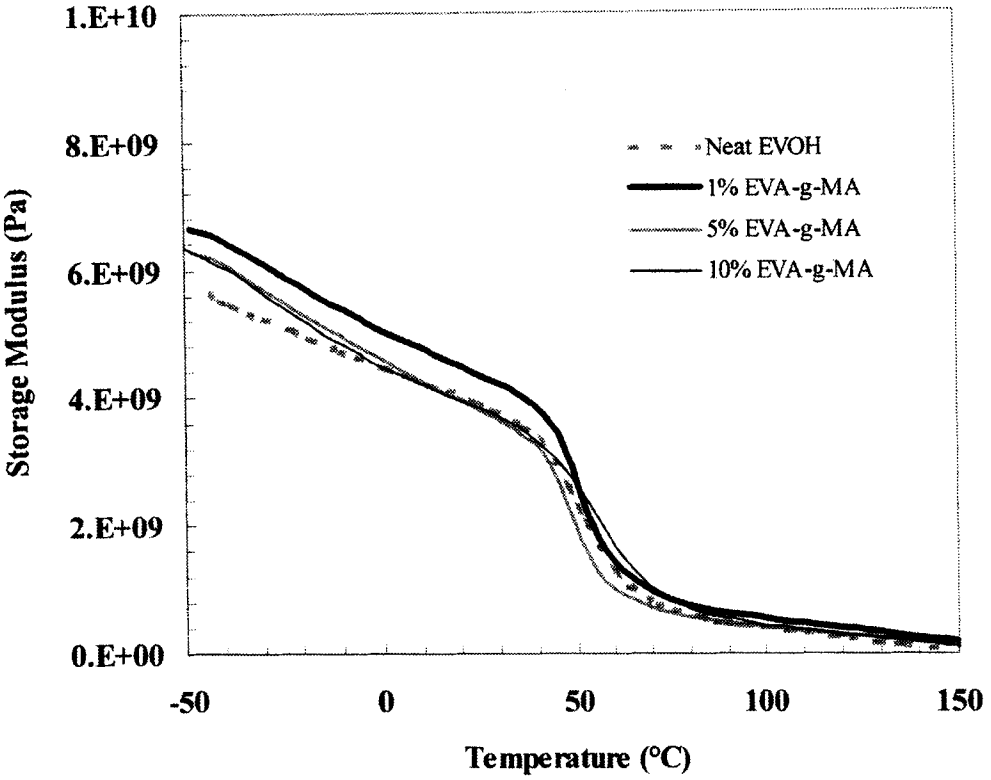

Fig. 6a. Storage modulus of EVOH containing EVA-g-MA.

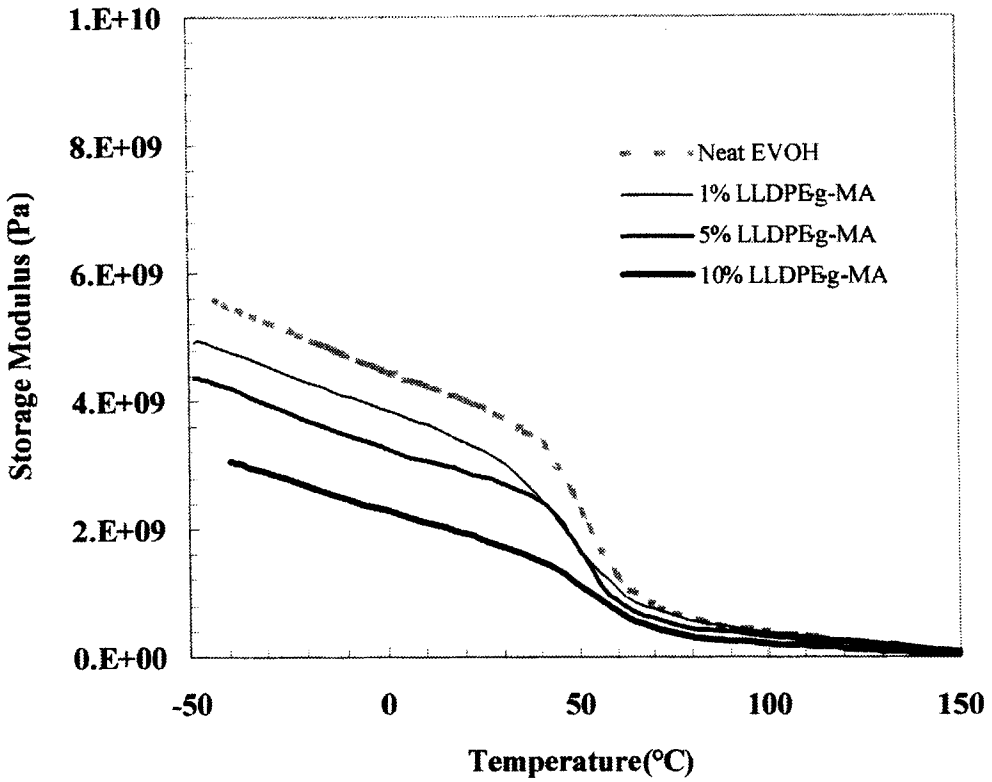

Fig. 6b. Storage modulus of EVOH containing LLDPE-g-MA.

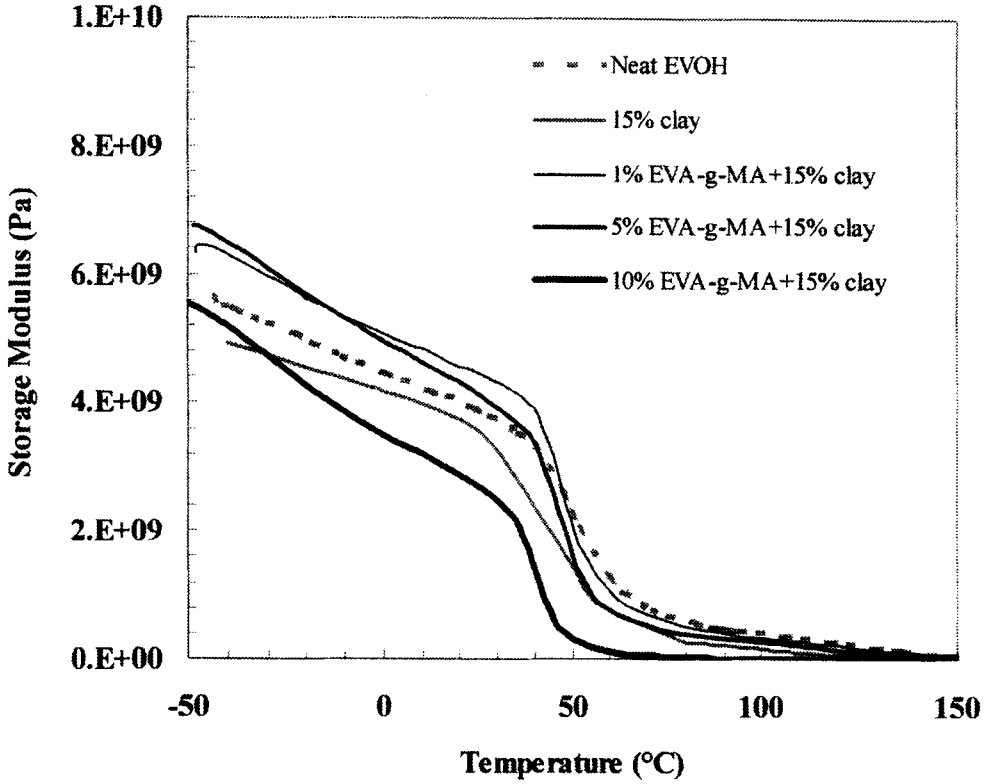

Fig. 7a. Storage modulus of EVOH/clay systems containing EVA-g-MA.

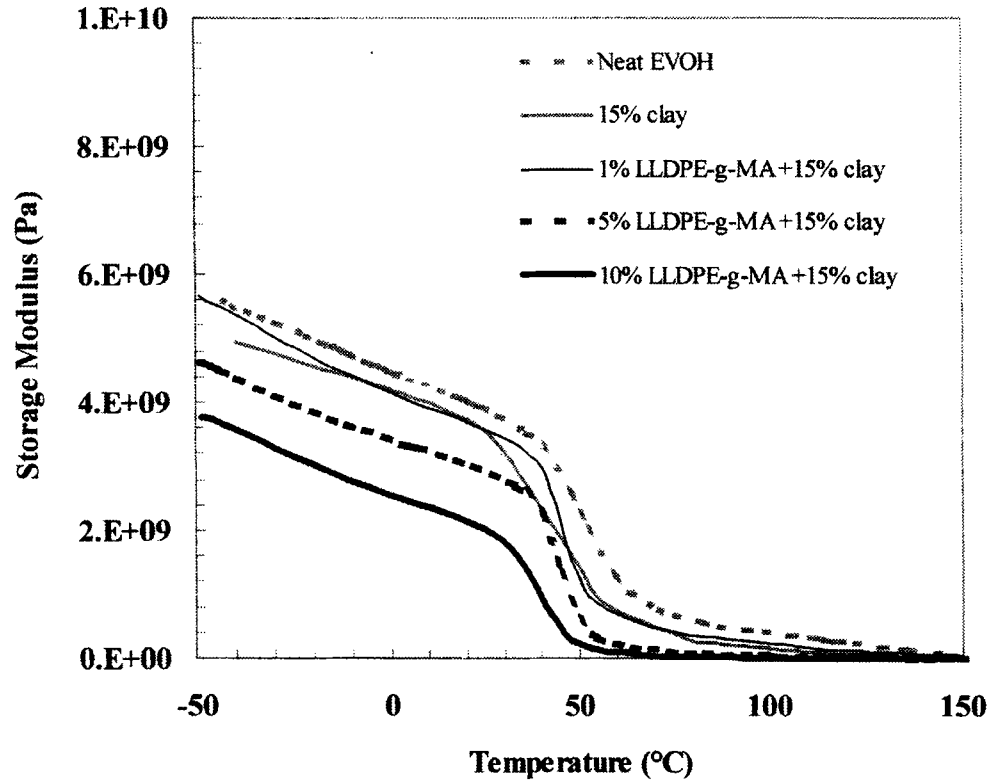

Fig. 7b. Storage modulus of EVOH/clay systems containing LLDPE-g-MA.

Table 2. DMTA T_g Values of EVOH/Clay/Compatibilizer Systems, Containing Different Amounts of Compatibilizers.

	T_g (°C)	
	EVA-g-MA	LLDPE-g-MA
Neat EVOH	50	50
15% E-clay	50	50
15% E-clay + 1% compatibilizer	52	50
15% E-clay + 5% compatibilizer	51	47
15% E-clay + 10% compatibilizer	41	39

Table 3. TGA Results of EVOH/Clay/Compatibilizer Systems, Containing Different Amounts of Compatibilizers.

	Temperature @ 50 wt% weight loss (°C)	
	EVA-g-MA	LLDPE-g-MA
Neat EVOH	404	404
Neat compatibilizer	415	394
15% E-clay	424	424
1% compatibilizer	414	415
15% E-clay + 1% compatibilizer	427	427
5% compatibilizer	410	410
15% E-clay + 5% compatibilizer	433	435
10% compatibilizer	412	415
15% E-clay + 10% compatibilizer	454	447

Table 4. Summary of the Main Results.

	EVA-g-MA		LLDPE-g-MA
Brabender data	**EVOH without clay**		
	Constant torque with time		
	1 wt%-highest torque (viscosity) 5 and 10 wt%-torque decreases gradually to its original value	>	1 wt%-highest torque (viscosity) 5 and 10 wt%-torque decreases gradually to its original value
	$\eta_{EVA\text{-}g\text{-}MA} < \eta_{EVOH}$		$\eta_{LLDPE\text{-}g\text{-}pMA} \cong \eta_{EVOH}$
	EVOH with 15 wt% clay		
	Torque increases with time		
	Shorter times for torque upturn with increasing EVA-g-MA content		Shorter times for torque upturn with increasing LLDPE-g-MA content
	10 wt% EVA-g-MA-mechanical degradation		5 and 10 wt% LLDPE-g-MA-mechanical degradation
X-ray: gallery heights	d_{001} (clay) = 25Å d_{001} (EVOH + 15 wt% clay) = 32Å d_{001} (EVA-g-MA + 15 wt% clay) = 42Å		d_{001} (LLDPE-g-MA + 15 wt% clay) = 29Å
	EVOH/clay/compatibilizer		
	1 wt%-d_{001} = 33Å 5 wt%-d_{001} = 35Å 10 wt%-d_{001} = 38Å		1 wt%-d_{001} = 34Å 5 wt%-d_{001} = 35Å 10 wt%-d_{001} = 38Å
SEM	**EVOH without clay**		
Freeze-fractured samples	Small EVA-g-MA spheres dispersed in the EVOH matrix		Large LLDPE-g-MA spheres dispersed in the EVOH matrix
	Spheres become larger with increasing compatibilizer content		
	EVOH with 15 wt% clay		
Freeze-fractured samples	Clay is hard to distinguish		
Microtomed samples	Stretched fibrils are observed		
	Smaller clay particles		Larger clay particles

Table 4. Continued

DSC	**EVOH without clay**	
	No change in thermal properties for all compatibilizer concentrations	
	EVOH with 15 wt% clay	
	1 wt%-less interruption to the crystallization process, compared to that of no compatibilizer	
	5 wt%-more interruption to the crystallization process	5 wt%-no crystallization
	10 wt%-no crystallization	10 wt%-no crystallization
DMTA	**EVOH without clay**	
	1 wt%-T_g increases	1 wt%-T_g decreases
	5 wt%-same T_g value	5 wt%-same T_g value
	10 wt%-T_g decreases	10 wt%-same T_g value
	Storage modulus decreases with compatibilizer content, but higher than that of neat EVOH for all contents	Storage modulus decreases with compatibilizer content, and lower than that of neat EVOH for all contents
	EVOH with 15 wt% clay	
	T_g decreases with compatibilizer content	
	E′ (85/15 EVOH/clay) < E′ (Neat EVOH)	
	1, 5 wt%-modulus increases with compatibilizer concentration, compared to neat EVOH	1 wt%-modulus higher than that of EVOH containing 15 wt% clay but lower than that of neat EVOH
	10 wt%-modulus higher than that of EVOH containing 15 wt% clay but lower than that of neat EVOH	5, 10 wt%-lowest modulus, decreases for higher compatibilizer contents

at all compositions. The viscosity gradually decreases when compatibilizer contents higher than 1 wt% are used. When hydrogen bonds between EVOH and compatibilizer have been formed, the presence of "excess," still unbonded compatibilizer, having lower viscosity than the hydrogen bonded EVOH/compatibilizer, leads to the viscosity decrease. Further verification for the higher compatibility of EVA-g-MA compared to LLDPE-g-MA with the EVOH is seen in the SEM micrographs, *Fig. 3*; the compatibilizer is dispersed as spheres in the EVOH matrix, which are smaller in the case of EVA-g-MA (*Fig. 3a* compared to *3b*). The DMTA results show that the different interaction levels of the two compatibilizers with EVOH lead to an opposite effect on the storage modulus of the blends compared to that of the neat EVOH (*Fig. 6*). The compatibilizers are expected to lower the modulus of the blends, owing to their lower modulus, a phenomenon that will be more pronounced for higher compatibilizer contents. Indeed this process occurs in the case of LLDPE-g-MA. However, when EVA-g-MA is used, although the moduli decrease for EVA-g-MA contents higher than 1 wt%, the moduli are higher than that of the neat EVOH, for all studied EVA-g-MA contents. This reminds the phenomenon seen when low contents of plasticizers are added to certain polymers and increase their modulus and tensile strength, i.e., act as antiplasticizers (20).

The effect of the compatibilizers in EVOH/clay/compatibilizer systems is significant. The Brabender results (*Fig. 1*) showing the gradual viscosity increase, which is more pronounced in the presence of the compatibilizers, is indicative of more fracturing of the organoclay particles. The clay fractures into small aggregates and undergoes delamination processes. The improved interaction level between the EVOH and the clay when compatibilizers are added leads to significant rise in the viscosity and shorter times for torque upturn to occur. The viscosity decrease after more than 30 min of processing for higher contents of compatibilizer stems from the material's high rigidity, due to the increasing level of EVOH/clay interaction, which eliminates segments and chains from the flowing polymer melt, leading to mechanical degradation (18).

The clay gallery height increases when compatibilizers are used in the blends. The presence of more polar groups and the high interaction level in the systems lead to enhanced intercalation. Although the tendency of neat LLDPE-g-MA to intercalate is lower than that of EVA-g-MA, the gallery heights obtained are similar for both compatibilizers. When EVA-g-MA is added there may be a competition between the compatibilizer and the EVOH regarding the intercalation process. Therefore, in this case, probably EVA-g-MA is also intercalated and more EVOH remains outside the galleries compared to the content of EVOH outside

when LLDPE-g-MA is used. This is expected to affect the crystallization of EVOH which cannot crystallize in the galleries confined space.

Although no changes in thermal properties of EVOH in EVOH/compatibilizer systems were seen, significant changes have occurred when both clay and compatibilizer were incorporated. Surprisingly, when 1 wt% of either compatibilizer was used, the interruption to the crystallization process was less pronounced than without the compatibilizer, i.e. the EVOH/clay system (*Table 2*). Hence, in the case where 1 wt% EVA-g-MA was added, the EVOH crystallinity was slightly higher than that without compatibilizer. However, when increasing amounts of compatibilizers of either type are used, the interruption to the EVOH crystallization process is more pronounced until at a certain concentration no crystallization occurs. This stems from the high interaction levels developed between the EVOH and the clay in the presence of the compatibilizers, thus ultimately EVOH segments cannot crystallize.

EVOH, although a random copolymer, crystallizes owing to strong hydrogen bonding of relatively small hydroxyl groups. The unique behavior of EVOH includes a crystallization process, which is influenced by its sensitivity to crystallization conditions. EVOH chains attached to the platelets are partially hindered from participating in the flow process and crystallization. The clay may behave as a "low quality" nucleating agent; however, it hinders the crystallization process, owing to the high interaction level with EVOH (18). Moreover, the intercalation level increases for higher compatibilizer contents; therefore, more delamination and exfoliation occur, resulting in more dispersion of single platelets, which further reduces crystallization.

The higher interaction level in the system when compatibilizers are used can also be seen in the SEM micrographs (*Fig. 4*). Intensive clay fracturing during melt mixing in the presence of compatibilizers leads to particles that are beyond the SEM resolution and therefore barely observable. Moreover, the high interaction level between the polymer and the clay, in the presence of the compatibilizers, may lead to fracture paths within the matrix rather than at the polymer/clay interface. Highly stretched fibrils crossing the cracks have been formed by microtoming the samples at room temperature (*Fig. 5*). The observed voids may represent clay particles that have been pulled out by microtoming. One can assume by the void size that the clay particles are larger in the case of LLDPE-g-MA (*Fig. 5b*) compared with EVA-g-MA (*Fig. 5a*), owing to the lower level of fracturing in the Brabender cell in the latter case. The fibrils were formed upon shearing of the EVOH/compatibilizer blend. These fibrils may be the result of high local deformation of interparticle polymer layers.

The different interaction level of the compatibilizers with the EVOH and the fracturing level of the clay affect the storage moduli of the blends. The particle fracturing/delamination processes are accompanied by increased level of interactions in the system. This enhanced interaction results in two opposing effects on the storage modulus. The first, common in nanocomposites, increases the modulus because of the increased polymer/clay interaction. The second, unique to the currently studied EVOH matrix polymer, results in a modulus decrease because of the dramatic crystallinity drop, ultimately to its elimination. It is concluded, based on the comprehensive thermal analysis presented, that the degree of crystallinity plays a major role in the mechanical behavior of the currently studied EVOH nanocomposite systems.

Bearing in mind that in the EVOH/clay systems the clay has a dramatic effect on crystallinity, whereas in EVOH/compatibilizer pairs, no crystallinity change occurs, it is suggested that by creation of additional clay surfaces, further reduction of crystallinity results. In this regard, LLDPE-g-MA is more effective than EVA-g-MA in the reduction of the degree of crystallinity in the EVOH/clay composites. Hence, LLDPE-g-MA monotonically decreases the storage modulus with increasing content. In contrast, EVA-g-MA initially increases the modulus and subsequently at higher contents decreases the modulus. The difference between the two compatibilizers in their effect on crystallinity and the derived mechanical properties is not obvious. It is suggested that LLDPE-g-MA presence results in more crystallinity, depressing "bare" clay surfaces than the EVA-g-MA. This is because the latter is a better intercalant, and the former is therefore at a higher content in the matrix, external to the clay particles. Since LLDPE-g-MA interaction with clay is lower than that of EVA-g-MA, more bare clay surfaces are available for interaction with EVOH. This clay/EVOH interaction is responsible for the reduction in crystallinity, as shown in *Tables 1* and *4*.

The compatibilizer plays an important role in determining the thermal stability of the blends (*Table 3*). The clay platelets have a shielding effect, lowering the oxygen supply rate, and thus slowing the rate of mass loss. When different amounts of compatibilizer are added in addition to the 15 wt% clay, the decomposition temperatures increase significantly for both compatibilizers. The increase is slightly higher when EVA-g-MA was used because of its larger effect on the level of delamination. The improvement in thermal stability when compatibilizers are used is in agreement with the advanced intercalation, based on the X-ray results, for the compatibilized blends. The maximum increase of decomposition temperature, compared to the neat polymer, i.e. 50°C, has occurred for the [75/15/10 EVOH/clay/EVA-g-MA] system.

The dramatic effect of interactions in the EVOH/clay/compatibilizer nanocomposites makes it a unique system that behaves significantly differently from the other known semicrystalline based polymer nanocomposites.

CONCLUSIONS

- The addition of compatibilizers enhances the intercalation levels of EVOH into clay galleries.

- Compatibilizers by themselves intercalate into clay galleries.
- T_m, T_c and degree of crystallinity of the EVOH in the presence of clay decrease with increasing compatibilizer content, until at certain content no crystallization takes place, owing to the high intercalation level of the EVOH, exfoliation of the clay and interactions between EVOH and clay in the presence of compatibilizer.
- Competition between the reinforcing effect of the clay platelets and crystallization depression determines the mechanical behavior of EVOH/clay/compatibilizer nanocomposites.
- The compatibilizer type, owing to different interaction levels with EVOH, shows different effects on the mechanical behavior of the composites: modulus enhancement with increasing compatibilizer content, followed by modulus reduction in the case of EVA-g-MA and gradual modulus decrease for LLDPE-g-MA.
- Improved thermal stability of the compatibilized blends was demonstrated by TGA, owing to advanced levels of intercalation/exfoliation.

ACKNOWLEDGMENT

The authors are grateful to the Israel Ministry of Science and Culture for partially supporting the nanocomposite project. N. Artzi acknowledges the generous Levi Eshkol scholarship (Israel Ministry of Science and Culture).

REFERENCES

1. G. Lagaly in *Development in Ionic Polymers*, A. D. Wilson and H. T. Posser, eds., Applied Science Publishers, London (1986).
2. A. Akelah in *Polymers and Other Advanced Materials*, N. Prasad, J. E. Mark, and T. J. Fai, eds., Plenum Press, New York (1995).
3. E. P. Giannelis, *Adv. Mater.*, **8**, 29 (1996).
4. T. J. Pinnavaia, T. Lan, Z. Wang, H. Shi, and P. D. Kaviratna, in *Nanotechnology*, G. M. Chow and K. E. Gonsalves, eds., American Chemical Society, Washington, D.C. (1996).
5. C. Zlig, P. Reichert, F. Dietsche, T. Engelhardt, and R. Mülhaupt, *Kunststoffe*, **88**, 1812 (1998).
6. P. Reichert, H. Nitz, S. Klinke, R. Brandsch, R. Thomann, and R. Mülhaupt, *Macromol. Mater. Eng.*, **275**, 8 (2000).
7. P. C. LeBaron, Z. Wang, and T. J. Pinnavaia, *Appl. Clay Sci.*, **15**, 11 (1999).
8. Z. Liang and H. L. Williams, *J. Appl. Polym. Sci.*, **44**, 699 (1992).
9. S. S. Dagly, M. Xhantos, and J. A. Biesenberger, *Polym. Prepr.*, **32**, 150 (1991).
10. N. R. Demarquette and M. R. Kamal, *J. Appl. Polym. Sci.*, **70**, 75 (1998).
11. J. B. Faisant, A. Ait-Kadi, M. Bousmina, and L. Deschenes, *Polymer*, **39**, 533 (1998).
12. K. S. Costas and K. K. Nikos, *Polymer*, **39**, 3863 (1998).
13. J. M. Willis, V. Caldas, and B. D. Favis, *J. Mat. Sci.*, **26**, 4742 (1991).
14. J. Villalpando-Olmos, S. Sánchez-Valdes, and I. G. Yáñez-Flores, *Polym. Eng. Sci.*, **39**, 1597 (1999).
15. N. Hasegawa, M. Kawasumi, M. Kato, A. Usuki, and A. Okada, *J. Appl. Polym. Sci.*, **67**, 87 (1996).
16. C. Zlig, R. Thomann, J. Finter, and R. Mülhaupt, *Macromol. Mater. Eng.*, **280/281**, 41 (2000).
17. N. Artzi, Y. Nir, M. Narkis, and A. Siegmann, *J. Polym. Sci., Part B: Polym. Phys.*, **40**, 1741 (2002).
18. N. Artzi, Y. Nir, D. Wang, M. Narkis, and A. Siegmann, *Polym. Compos.*, **22**, 710 (2001).
19. Y. Nir, M. Narkis, and A. Siegmann, *J. Polym. Sci., Part B: Polym. Phys.*, **38**, 813 (2000).
20. M. Shuster, M. Narkis, and A. Siegmann, *Polym. Eng. Sci.*, **34**, 1613 (1994).